Superstructure and Mechanical Properties of Poly(ethylene terephthalate) Fibers Zone-Drawn Under Critical Necking Tension

AKIHIRO SUZUKI, TAKASHI KAWADA

Department of Applied Chemistry and Biotechnology, Faculty of Engineering, Yamanashi University, 4-3-11 Takeda, Kofu, 400-8511 Japan

Received 21 December 2000; accepted 13 April 2001

ABSTRACT: The superstructure and mechanical properties of poly(ethylene terephthalate) fibers zone-drawn under a critical necking tension (σ_c) were studied. σ_c was defined as the minimum tension needed to generate a neck at a given drawing temperature (T_d) and was measured over a temperature range of 70–120°C. The σ_c value increased rapidly with decreasing T_d in the temperature range below 85°C, but the temperature dependence of σ_c was small above 85°C. The neck profile relied on T_d, becoming more shapely with decreasing T_d. A neck with a gradual decrease in diameter was observed in the fibers drawn at 100°C and above. The draw ratio increased significantly with increasing T_d above 90°C, but birefringence decreased. Density decreased gradually with increasing T_d, and fiber drawn at 120°C had a density of 1.347 g/cc. Wide-angle X-ray diffraction photographs of the fibers drawn at 100°C and below showed reflections due to crystallites, but a photograph of the fiber obtained at 120°C showed a ring-like amorphous halo. The storage modulus (E') at 25°C increased progressively with decreasing T_d, and the fiber drawn at 70°C had the maximum E' value among the fibers drawn at a series of T_d's. © 2002 John Wiley & Sons, Inc. J Appl Polym Sci 83: 179–185, 2002

Key words: poly(ethylene terephthalate) fibers; zone drawing; necking; critical necking tension; orientation; WAXD

INTRODUCTION

In the drawing processes of many polymers, necking is induced in a very narrow temperature range close to the glass-transition temperature (T_g) and plays an important role in the production of polymers with high moduli and high strength. Necking in amorphous and semicrystalline polymers has been studied extensively.[1–6]

Zone drawing[7–10] is carried out by the movement of a zone heater along the drawing direction at a constant speed. The zone heater gives a sharp temperature distribution, and a stable neck occurs easily when heated locally without any initiation of the neck. The neck induced in the zone heater is propagated by movement of the zone heater at a constant speed. Because the zone drawing can readily induce the neck in a wide temperature range, the method is convenient for the study of neck behavior as compared to other normal drawings.

We already reported, in the zone-drawing processes of fibers and films, that the necking was observed over a wide temperature range and that

Correspondence to: A. Suzuki (a-suzuki@ab11.yamanashi.ac.jp).

Journal of Applied Polymer Science, Vol. 83, 179–185 (2002)

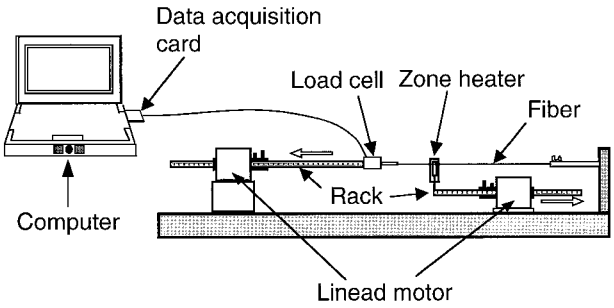

Figure 1 Schematic diagram of the instrument used for the measurement of σ_c.

the neck geometry depended strongly on the drawing condition.[11–13] Because zone drawing readily induces the neck even at a temperature sufficiently above T_g, it is convenient to study the superstructure induced by necking over a wide temperature range.

The purpose of this investigation was to study the superstructure and mechanical properties of poly(ethylene terephthalate) (PET) fibers zone-drawn under a critical necking tension (σ_c). σ_c was defined as the minimum tension needed to generate necking at a given drawing temperature (T_d).

EXPERIMENTAL

Material

The original material used in this study was as-spun PET fibers supplied by Toray Ltd. (Japan). The as-spun fiber had a diameter of about 0.25 mm, a density of 1.339 g/cc, and a birefringence (Δn) of 1.1×10^{-3}.

Apparatus for the Measurement of σ_c

Measurements of σ_c were carried out with the apparatus shown schematically in Figure 1. This apparatus consisted of a temperature-controlled zone heater, a load cell connected to a microcomputer through a data-acquisition card, and two speed-control motors capable of moving the zone heater and a load cell at an arbitrary speed. The speed-control motor had a linear head that converted rotational motion of the motor into linear motion. One end of the fiber was attached to a jaw equipped with the load cell, and the other was run through the zone heater and fixed at the jaw, fastened to a frame. The data via the data-acquisition card were stored in the microcomputer at an interval of 50 ms.

To determine σ_c at a given T_d, a stress versus drawing time curve at each T_d was recorded at a drawing speed of 50 mm/min and a zone-heater speed of 10 mm/min. Figure 2 shows a schematic illustration of the stress versus drawing time curve. The stress increased rapidly with the drawing time and then reached a yield point. The neck was formed at the yield point and propagated along the fiber by the movement of the heater. The yielded value in the onset point of the neck was defined as the σ_c.

Measurement

The draw ratio (λ) was determined in the usual way by measurement of the displacement of ink marks placed 10 mm apart on the film prior to drawing.

Δn was measured with a polarizing microscope equipped with a Berek compensator (Olympus Optical Co. Ltd., Japan). A X-Z quartz compensator cut from a single crystal was also used because the drawn PET fiber had a higher retardation. The density of the fiber was measured at 23°C by a flotation technique with a carbon tetrachloride and toluene mixture.

The neck profiles of the fibers drawn at various T_d's were photographed with a polarized microscope equipped with a camera.

Wide-angle X-ray diffraction (WAXD) data were obtained on a Rigaku diffractometer (Rigaku Co., Japan) with Ni-filtered CuK$_\alpha$ (wavelength = 1.542 Å) radiation generated at 40 kV and 20

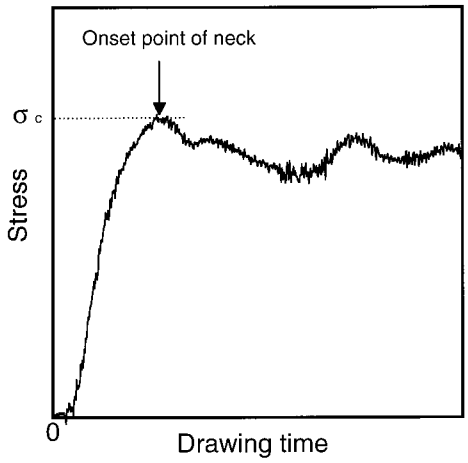

Figure 2 Schematic illustration of the stress–time curve.

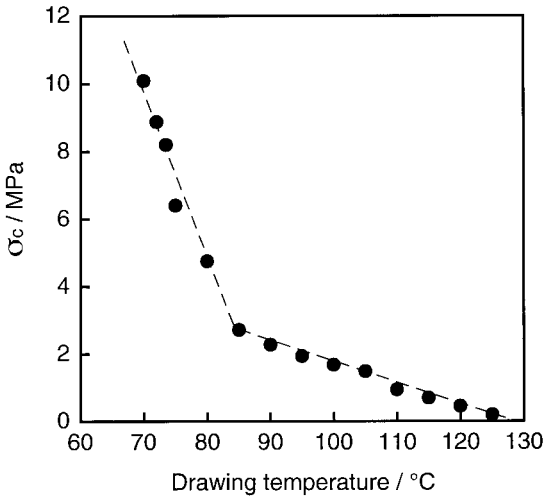

Figure 3 Change in the σ_c with T_d.

mA. Scattered X-rays were measured with a scintillation counter. WAXD photographs of the fibers were taken with a flat-film camera. The camera was attached to a Rigaku X-ray generator, which was operated at 36 kV and 18 mA. The radiation used was Ni-filtered CuK_α. The sample-to-film distance was 40 mm. The fiber was exposed for 4 h to the X-ray beam from a pinhole collimator with a diameter of 0.4 mm.

A Tensilon tensile testing machine (Orientec Co. Ltd., Japan) was used to determine tensile modulus, tensile strength, and elongation at break. A gauge length of 5 cm and an elongation rate of 10 mm/min were used. The experimental results were the average of 10 measurements.

The dynamic viscoelastic properties were measured at 110 Hz with a dynamic viscoelastometer (VIBRON DDV-II, Orientec). Measurements were carried out over a temperature range of 25°C to about 225°C at an interval of 5°C, and the average heating rate was 2.5°C/min. The strip was held at a 20-mm gauge length between two jaws.

RESULTS AND DISCUSSION

Neck Profile of Fiber Zone-Drawn Under σ_c

To study the relation between the neck profile and drawing condition, the as-spun PET fiber was drawn under various σ_c's. Zone drawing under σ_c can induce the neck over a wide temperature range.

Figure 3 shows the change in σ_c with T_d. The σ_c value decreased rapidly with increasing T_d up to 85°C; above this value, the decrease in σ_c was small. At 85°C and above, the σ_c was a low value of about 2 MPa or less. The fiber could not be

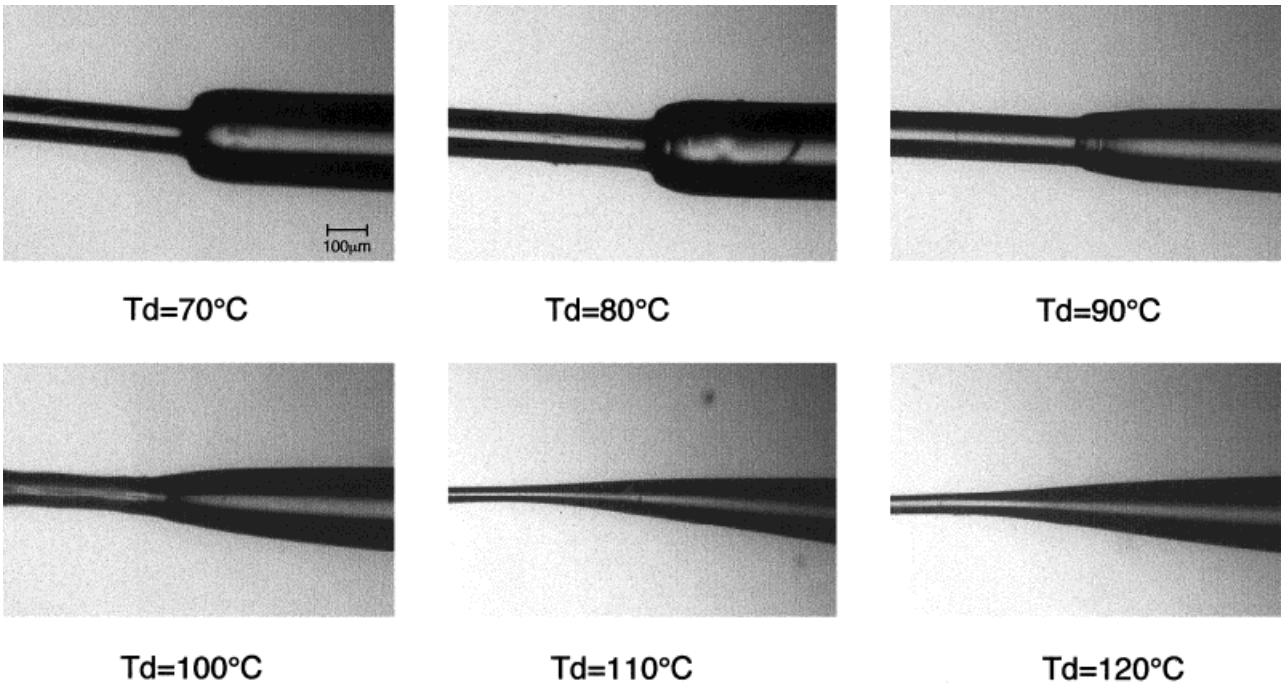

Figure 4 Microphotographs of the neck profiles of the fibers drawn at various T_d's.

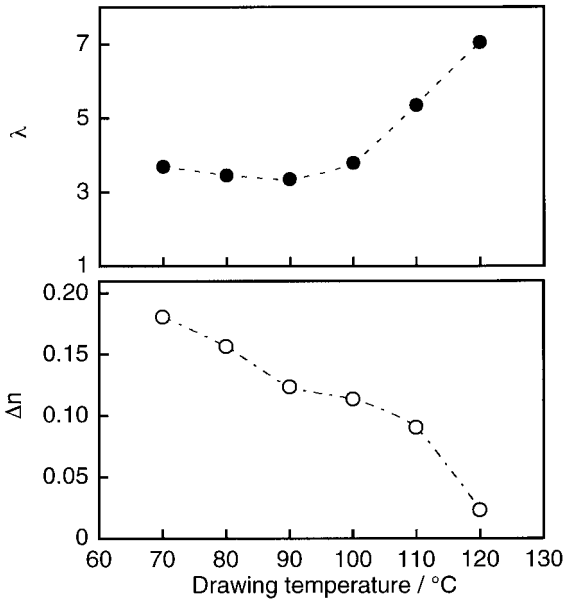

Figure 5 Changes in λ and Δn with T_d.

drawn below 70°C, and σ_c values above 120°C were not obtained because no obvious yield point was observed in the stress versus drawing time curve.

Figure 4 shows microphotographs of the neck profiles of the fibers drawn at various T_d's. Neck profiles of the zone-drawn fibers depended strongly on T_d and became more shapely with decreasing T_d, and the necking zone narrowed at a lower T_d. The fiber drawn at 70°C had the steepest shoulder among the fibers drawn at a series of T_d's. The fibers drawn at 100°C and above showed a neck with a gradual decrease in diameter. The diameters of fibers drawn at 110 and 120°C were obviously thinner than those of the fibers drawn at lower T_d's.

Figure 5 shows the changes in λ and Δn with T_d. λ decreased slightly with increasing T_d up to 90°C, but above this, the value of λ increased significantly with increasing T_d. On the other hand, Δn decreased with increasing T_d, and the fiber with the highest λ had the lowest Δn (0.023). The maximum Δn (0.181) was at T_d = 70°C. This shows that the drawing carried out at T_d = 70°C gave the highest drawing efficiency and that in the drawing at T_d above 100°C, the chain-slippage process predominated over the orientation process.

Figure 6 shows density plotted against the T_d. The density decreased gradually with increasing T_d, and the fiber drawn at 120°C has a density of 1.347 g/cc. The maximum density was given by

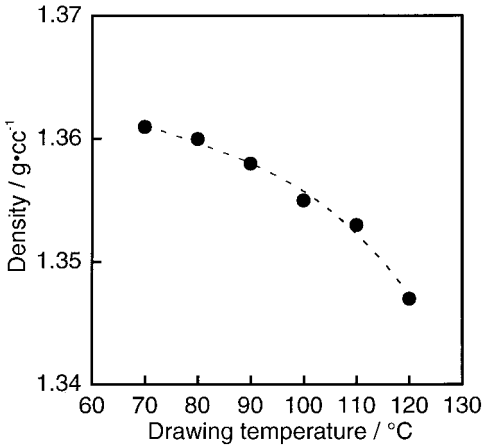

Figure 6 Change in density with T_d.

the fiber drawn at 70°C and was 1.361 g/cc. The maximum value was lower than that (1.369 g/cc) of the zone-drawn PET fiber reported previously.[14] An apparent lowering of the density meant that the strain-induced crystallization hardly occurred at higher T_d's.

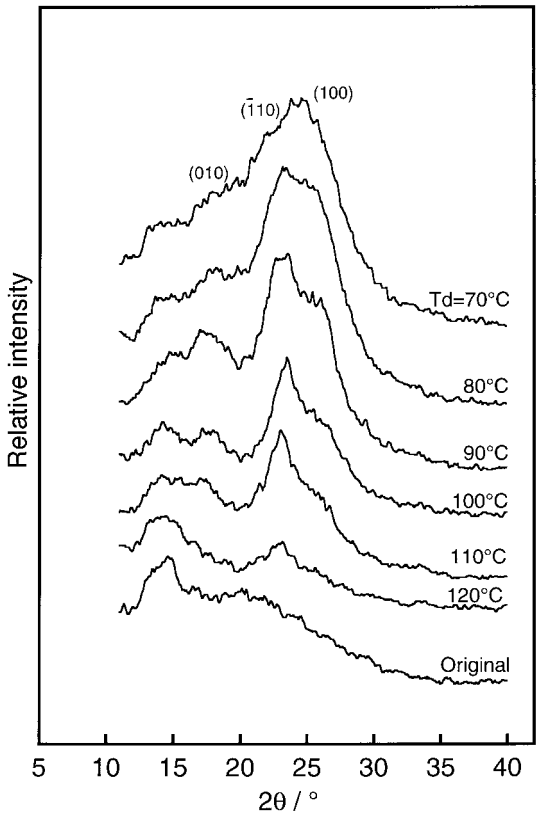

Figure 7 WAXD equatorial patterns of the original fiber and the fibers drawn at different T_d's.

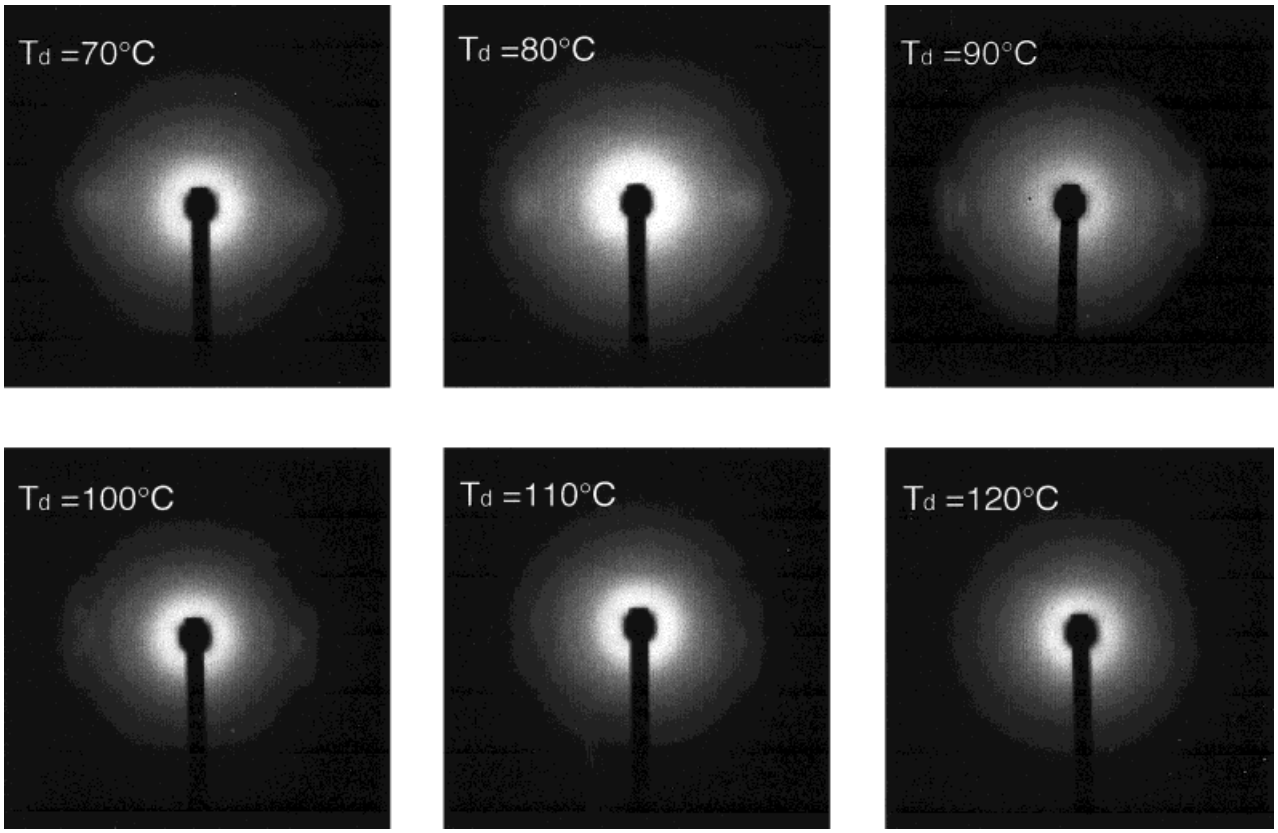

Figure 8 WAXD photographs of the fibers drawn at six different T_d's.

Figures 7 and 8 show the WAXD equatorial patterns and the WAXD photographs for the original fiber and the fibers obtained at six different T_d's. These equatorial patterns were poorly resolved patterns. In the WAXD patterns of the PET fiber,[14] three reflections, (010), ($\bar{1}$10), and (100), were observed in the equator. However, the individual diffraction peaks were not clearly present in Figure 7, and a double peak hardly separated into reflections due to the ($\bar{1}$10) and (100) plates. The WAXD photographs of the fibers drawn at 100°C and below showed faint reflections due to crystallites. The poorly resolved patterns suggest that the crystallites formed by the drawing under σ_c were smaller and imperfect. The photographs of the fibers obtained at 110 and 120°C did not give any reflections and showed a ring-like amorphous halo.

The results suggest that in the zone drawing carried out at the higher T_d, the chain-slippage processes predominated over the molecular orientation process and the strain-induced crystallization. Consequently, the σ_c dropped to a low level, which resulted in flow drawing and caused a large deformation without induction of molecular orientation and crystallization.

Mechanical Properties of the Fibers Drawn Under σ_c

Table 1 lists the tensile modulus, tensile strength, and elongation at break of the original fiber and the fibers zone-drawn at a series of T_d's. The tensile modulus increased stepwise with decreasing T_d, and the fiber drawn at 70°C had a maximum tensile modulus of 9.2 GPa. However, a maximum tensile strength of 0.77 GPa was given by the fiber drawn at 90°C. In the zone-annealed PET fiber reported previously,[14] the fiber with the maximum modulus had the maximum strength. Unlike the zone-annealed PET fiber, the fiber drawn at 70°C did not have the maximum strength, although it had the maximum modulus. The result implies that the mechanical properties of the fiber drawn at T_d = 90°C was improved by a strain hardening induced during the tensile testing because its elongation at break was 120%.

Figure 9(a) shows the temperature dependence of the storage modulus (E') for the original fiber

and the fibers drawn at a series of T_d's. The E' of the fibers, except the fibers drawn at 110 and 120°C and the original fiber, decreased gradually with increasing temperature and more rapidly in the temperature range from 70 to 150°C. The E'–temperature curves above 200°C were indistinguishable from each other. Viscoelastic properties of the original fiber and the fibers drawn at 110 and 120°C could not be measured up to higher temperature because of the fluid-like deformation due to chain slippage. The flow deformation indicates that the network built up the crystallites with lower perfection and crystalline nuclei and the molecular entanglements were thermolabile at the higher temperature.

Figure 9(b) shows the temperature dependence of the loss tangent (tan δ) for the original fiber and the fibers drawn at a series of T_d's. The fibers, except the fiber drawn at 120°C, show α peaks in the temperature range of 100–135°C, which were considered to originate from the glass transition. The α peak shifted to a higher temperature, decreased in its peak height, and became much broader with decreasing T_d. The changes in position and in the profile of the dispersion peak attributed to glass transition (α peak) with T_d point out that the molecular mobility in the amorphous regions was restricted by the surrounding crystallites.

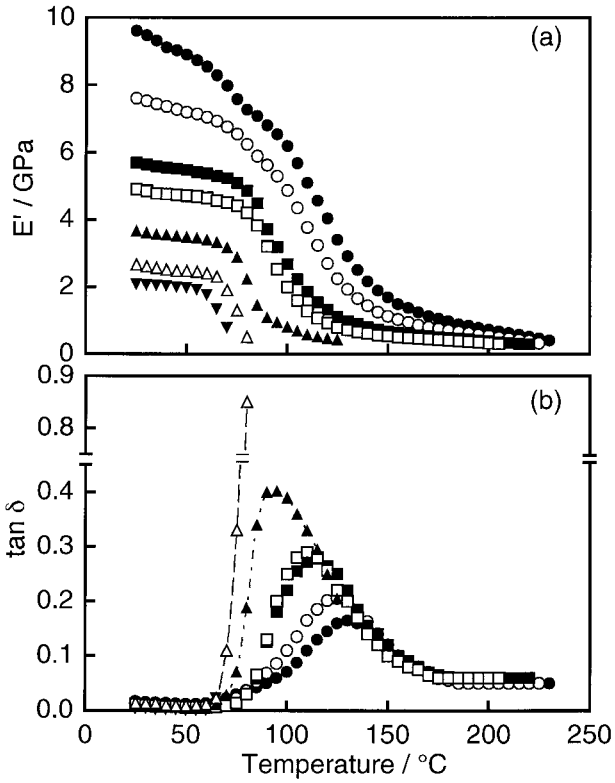

Figure 9 Temperature dependence of (a) E' and (b) tan δ for the fibers obtained at various T_d's: (●) 70, (○) 80, (■) 90, (□) 100, (▲) 110, and (△) 120°C and (▼) original fiber.

CONCLUSIONS

The as-spun PET fibers were zone-drawn under various σ_c's. σ_c decreased rapidly with increasing T_d up to T_d = 85°C, above which value the change in σ_c with T_d was small. Δn and the density decreased with increasing T_d, but λ increased rapidly with increasing T_d above 100°C. The neck profile depended on the T_d, becoming more shapely with decreasing T_d. The fibers drawn at 70 and 80°C had a neck with a steeper shoulder, but the fibers obtained at 100°C and above had an extended neck.

The zone drawings under σ_c at 90°C and below induced crystallization and molecular orientation. On the other hand, the zone drawings under σ_c at 100°C and above resulted in a large deformation hardly accompanied with crystallization and molecular orientation.

Table I Tensile Properties for the Original Fiber and the Fibers Obtained at Various T_d's

Fiber Drawn at T_d (°C)	Tensile Modulus (GPa)	Tensile Strength (GPa)	Elongation at Break (%)
Original	2.3	—	—
70	9.2	0.58	57
80	7.4	0.72	84
90	5.5	0.77	120
100	4.8	0.65	119
110	3.8	0.55	136
120	2.7	0.53	194

We are grateful to Toray for supplying us with PET fibers.

REFERENCES

1. Nazarenko, S.; Bensason, S.; Hiltner, A.; Baer, E. Polymer 1994, 35, 3883.
2. Matques, A.; G'Sell, C.; Neale, K. W. Polymer 1989, 30, 636.
3. Hristov, H. A.; Hearle, J. W. S.; Schultz, J. M.; Kennedy, A. D. J Polym Sci Part B: Polym Phys 1995, 33, 125.

4. Coate, P. D.; Ward, I. M. J Mater Sci 1978, 13, 1957.
5. Coate, P. D.; Ward, I. M. J Mater Sci 1980, 15, 2897.
6. Coate, P. D.; Gibson, A. G.; Ward, I. M. J Mater Sci 1978, 13, 1957.
7. Kunugi, T.; Suzuki, A.; Hashimoto, M. J Appl Polym Sci 1981, 26, 1951.
8. Kunugi, T.; Akiyama, I.; Hashimoto, M. Polymer 1982, 23, 1199.
9. Suzuki, A.; Kohno, T.; Kunugi, T. J Polym Sci Part B: Polym Phys 1998, 36, 1731.
10. Suzuki, A.; Kuwabara, T.; Kunugi, T. Polymer 1998, 39, 4235.
11. Kunugi, T.; Suzuki, A.; Hayakawa, T. Kobunshi Ronbunsyu 1991, 48, 703.
12. Suzuki, A.; Kobayashi, K.; Kunugi, T. Kobunshi Ronbunsyu 1993, 50, 205.
13. Suzuki, A.; Naito, M.; Kunugi, T. Kobunshi Ronbunsyu 1994, 51, 500.
14. Suziki, A.; Sato, Y.; Kunugi, T. J Polym Sci Part B: Polym Phys 1998, 36, 473.